Vol.67: e24231023, 2024
https://doi.org/10.1590/1678-4324-2024231023
ISSN 1678-4324 Online Edition

BABT
Brazilian Archives of Biology and Technology

Article - Engineering, Technology and Techniques

Bactericidal Effectiveness of 3D Printed PLA Surfaces Coated with Sealant Containing Silver Nitrate

Ully Guimarães Rocha[1]
https://orcid.org/0000-0001-8854-7462

Daniel José Nahid Mansur Chalhub[1*]
https://orcid.org/ 0000-0003-1956-5987

Norberto Mangiavacchi[1]
https://orcid.org/ 0000-0001-9555-9023

André Rocha Pimenta[2]
https://orcid.org/ 0000-0002-5492-3009

Marco Antônio Lemos Miguel[3]
https://orcid.org/0000-0002-6964-0749

Marília Garcia Diniz[1]
https://orcid.org/0000-0002-1836-8618

[1]Universidade do Estado do Rio de Janeiro, Departamento de Engenharia Mecânica, Rio de Janeiro, RJ, Brasil; [2]Instituto Federal do Rio de Janeiro, Departamento de Engenharia Mecânica, Rio de Janeiro, RJ, Brasil; [3]Universidade Federal do Rio de Janeiro, Instituto de Microbiologia Paulo de Góes, Rio de Janeiro, RJ, Brasil.

Editor-in-Chief: Alexandre Rasi Aoki
Associate Editor: Marcos Pileggi

Received: 06-Oct-2023; Accepted: 13-May-2024

*Correspondence: daniel.chalhub@eng.uerj.br; Tel.: +55 (21) 2332-4733 (D.J.N.M.C.).

HIGHLIGHTS

- In vitro tests were conducted to assess bactericidal effects on coated PLA surfaces
- Advanced techniques, including SEM, EDS, and OM, were utilized for detailed analysis.
- Sealed PLA surfaces reduce bacterial growth by over 64 times in just 30 minutes.
- The method's flexibility suggests applications across various materials and surfaces.

Abstract: This research characterized the morphological and chemical characteristics, as well as the biocidal effectiveness of polylactic acid (PLA) plate surfaces, created through additive manufacturing, both with and without an additional sealing coating of a polymer infused with silver nitrate crystals. In acknowledgement of the well-accepted principle of silver-based materials as antibacterial agents, this study delves deeper into the underlying mechanism responsible for the bactericidal effect of the sealant, offering a thorough characterization of the system and its behavior. To assess the bactericidal effect of the system, a suite of techniques including visual examination, optical microscopy (OM), digital image processing (DIP), scanning electron microscopy (SEM), semi-quantitative chemical analyses using energy dispersive spectroscopy (EDS), average roughness (Ra) computations, and *in vitro* tests were employed. The goal was to assess the impact of the presence or absence of the sealant on the proliferation of *Escherichia coli* American Type Culture Collection (ATCC) 11229 and *Staphylococcus aureus* ATCC 25923 bacteria. Results showed that the sealant had a significant antimicrobial effect, reducing the number of bacteria on the coated surfaces by at least 64 times within 30 minutes, in comparison with uncoated surfaces. This study also revealed the presence of micropores in the cross-section of the sealant layer. The microporous structure likely served as a conduit for silver ions from the encapsulated silver nitrate to exert their bactericidal effect on bacterial colonies. Whilst reinforcing the well-known bactericidal efficacy of silver, this investigation underscores the potential applicability of the proposed sealant in various fields requiring antimicrobial protection.

Keywords: PLA; additive manufacturing; biocidal inorganic sealant; silver; *in vitro* tests.

INTRODUCTION

The rapid international dissemination of viruses and bacteria can swiftly escalate localized epidemics into widespread pandemics [1]. Given the rise of novel viruses and increasingly resistant bacterial strains, there is a growing need for investigations into biocidal substances and the development of more efficacious protective equipment. In healthcare facilities, for instance, where the risk of contamination is heightened and the implementation of enhanced cleaning strategies can prove difficult, only a small fraction of surfaces undergoes satisfactory sanitization. This contributes to an environment favoring hospital infection scenarios [2]. In an attempt to combat proliferation caused by contamination of surfaces of stretchers, tables, switches, and hospital materials, numerous studies have evaluated the activity and biocidal effectiveness of metals such as copper [3,4], zinc, and silver, in pure or micro or nanostructured composite forms. In this context, silver has stood out as a biocidal agent [5,6].

Additive manufacturing, commonly known as 3D printing, has emerged as a highly effective method for producing industrial personal protective equipment (PPE) and various polylactic acid (PLA) items, including those utilized in hospitals [7]. Conversely, sealants serve as protective coatings on surfaces, functioning much like a paint scheme that fills pores and mitigates the effects of surface porosity, as they infiltrate these imperfections. These specialized paints enhance the protection of the underlying material by reducing its exposure to external factors. They work by adhering to the surface and may be formulated from epoxy resin, polyester, polyurethane, or wax. While sealants may or may not contain metallic pigments, their efficacy relies on several characteristics: low viscosity at application, minimal water absorption, compatibility with the operating environment, and a thin profile, typically no more than 75 µm [8].

Materials with antimicrobial properties are critically important in settings where cleanliness and hygiene are paramount. Therefore, creating materials with biocidal capabilities has proven to be an effective strategy to manage risk scenarios. Biocidal agents, often introduced as additives, have found their way into a variety of applications including food packaging, kitchen utensils, piping systems, air filters, containers, and medical products like gloves, catheters, dressings, and bed linens. However, further data on their efficacy, longevity of action, and operative mechanisms are still needed [9-11].

The aim of this study is to assess the biocidal effectiveness of a sealant derived from a polymer imbued with silver nitrate crystals, applied to the surface of Polylactic Acid (PLA) thermoplastic plates produced via 3D printing. This setup is designed to emulate the surface of hospital equipment manufactured using the same technique. While the bactericidal efficacy of silver is a well-established concept, this study seeks to delve deeper into the underlying mechanism responsible for the bactericidal effect of the sealant. The systems, both with and without the sealant, are analyzed using several characterization methods including optical microscopy (OM), average roughness (Ra) measurements, scanning electron microscopy (SEM), semi-quantitative chemical analysis through Energy Dispersive Spectroscopy (EDS), and digital image processing (DIP). In addition, the systems are evaluated through *in vitro* tests when exposed to the bacteria *Escherichia coli* ATCC 11229, a bacterium with a chemically complex cell wall, and *Staphylococcus aureus* ATCC 25923, which has a chemically simple cell wall. The tests evaluate the biocidal effect of the sealant on these microorganisms.

MATERIAL AND METHODS

A total of 100 PLA plates, each measuring 25 x 25 x 5 mm, were fabricated using additive manufacturing with a Sethi3D brand 3D printer, model BB, featuring a maximum printing volume of 400mm x 400mm x 400mm. The fabrication process utilized PLA from a consistent batch, and the printing parameters were set as follows: a printing speed of 35 mm/s, a temperature of 210 °C, layer height of 0.30mm, line width of 0.48mm, two walls, three base layers, and three top layers. The fabrication parameters selected for this study align with standard practices in 3D printing and are also recommended settings for this type of 3D printer, facilitating optimal print quality and structural integrity in PLA-based additive manufacturing.

The sealant was formulated using Revell brand varnish, model VER 32101, and solid silver nitrate ($AgNO_3$) crystals from the ACS brand, ensuring analytical purity (AP). A mixture ratio of 1mL of varnish to every 0.1g of silver nitrate was prepared, ensuring a homogeneous suspension of the crystals within the varnish. The distribution of silver nitrate particles is achieved through a manual mechanical mixing process. The dispersion of these particles is influenced by their individual sizes and the specific mechanics of the manual mixing technique. This mixture was then applied in a single coat to one side of the PLA plates using a manual technique with a Tigre brand brush, model number 267-6, without a specific alignment to the

direction of PLA printing. Following a drying period of 24 hours, both visual inspection and qualitative analysis were employed to verify the successful adhesion of the silver nitrate crystals to the PLA surface. Although the coating process aims for uniformity, the distribution of silver nitrate crystals does exhibit particle agglomeration patterns also known as clusters — a characteristic inherent to the mechanism of mechanical mixing and application. As a single coat was applied to all samples, they all have the same average coating thickness. Figure 1 depicts the appearance of a printed PLA plate after the application of the sealant, illustrating the successful integration of the silver nitrate crystals within the varnish layer and their adhesion to the substrate.

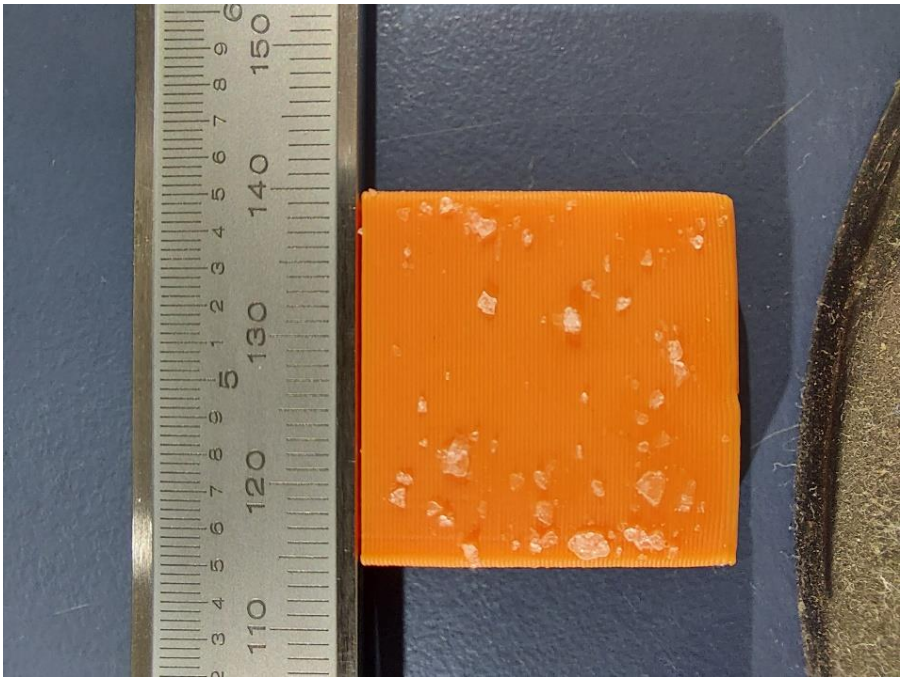

Figure 1. PLA plate coated with the sealant, 24 hours after the application of the varnish and silver nitrate crystals mixture.

Average roughness (Ra) measurements were taken using a Mitutoyo digital roughness meter, model SJ210, featuring a 5 µm radius probe tip and equipped with the ST Communication Tool software. For the testing procedures, parameters were implemented in accordance with the standards specified in ABNT NBR ISO 4288:2008 and ABNT NBR ISO 4287:2002 [12,13].

Analyses were conducted on ten uncoated plate surfaces and five surfaces coated solely with varnish. Given that the vertical measuring capacity of the roughness meter was limited to 100 µm, measurements were taken only on surfaces without silver nitrate crystals, as some crystals exceeded this size. For each plate, two measurements were made: one parallel to the direction of the print lines and another perpendicular, to assess the degree of anisotropy of the material surface [14].

Optical microscopy (OM) images of all produced surfaces were captured using an Olympus microscope, model 8ZX16. Scanning electron microscopy (SEM) was performed using a Hitachi TM3000 microscope, operating at 15kV in backscattered electron mode (BSE). To analyze the cross-section of the sealant coating layer, samples were fractured following immersion in liquid nitrogen (-196.15 °C), and subsequently coated with a 2 µm layer of chromium ions [15] for observation through a JEOL JSM 7100F Field Emission Gun (FEG) SEM. In addition, chemical microanalysis of the surfaces was carried out using a Bruker EDS detector, model X Flash MIN SVE, integrated with the TM3000 SEM model.

Digital image analysis and processing (DIP) was employed to estimate the area fraction (AA %) or volumetric fraction (Vv %) occupied by silver nitrate crystals on the plates coated with the sealant [16]. This was carried out using the FIJI Image J software, version 2.0, and leveraging color segmentation techniques [17]. Ten images of the coated plate were processed, all at a magnification level of three times.

The *in vitro* tests utilized microorganisms stored at 4°C in Tripticasein soy agar (TSA) supplied by the Kasvi brand [18]. Two representative types of bacteria commonly used in public health studies were employed: a Gram-negative strain (*Escherichia coli* ATCC 11229) and a Gram-positive strain (*Staphylococcus aureus* ATCC 25923) [19]. The bacteria were propagated in a chemically complex and

nutritionally rich culture medium (Brain and Heart Infusion - BHI) solidified with agar, which allows the full multiplication of the bacteria used.

Following inoculation, they were placed in a 37 °C incubator for 24 hours to encourage the development of Colony-Forming Units (CFUs). CFUs are a measure used in microbiology to estimate the number of viable bacteria or fungal cells in a sample [20]. Each unit denotes a site where a single viable cell has multiplied into a visible colony. From the colonies obtained, a bacterial suspension containing 3×10^8 CFU/mL (colony forming units per milliliter of solution) was prepared, using the McFarland scale 1 as a reference, which is a chemical turbidity scale that corresponds to the turbidity obtained with this concentration of microorganisms and normally used in laboratory practice in microbiology [21-24].

The surfaces tested for bactericidal action underwent disinfection with 70% ethanol (vol/vol) and exposure to Ultraviolet (UV) radiation for 15 minutes. All tools utilized in the experiments were likewise disinfected with ethanol and UV, and additionally autoclaved at 121°C for 15 minutes to ensure complete sterilization [25]. Tests were conducted thrice for each type of bacteria. Each test involved inoculating 10µL of the saline solution containing bacteria at the McFarland 1 standard onto three different surfaces:

- Pure PLA plates: PLA plates without any coating (serving as the control),
- Varnished PLA plates: PLA plates coated solely with varnish (absent of silver nitrate), and
- Sealed PLA plates: PLA plates coated with the sealant (comprising a blend of varnish and silver nitrate).

PLA plates coated solely with varnish (absent of silver nitrate) were included in the test set to ascertain whether the varnish alone exerted any bactericidal effect. This experimental design allowed for the isolation of the potential antimicrobial activity of the varnish from that of silver nitrate. Each test plate was estimated to be exposed to approximately three million colony-forming units (CFUs) of bacteria [19]. Thirty minutes following this exposure, the plates were immersed in 5 mL of saline solution and brushed gently for one minute to detach the bacteria from the surfaces and transfer them into the saline solution. Subsequently, 10 µL of this solution was added to 20 mL of BHI present in petri dishes. After executing this procedure for both strains of bacteria and all tested surface conditions, the petri dishes were placed in an incubator at 37°C for 24 hours. Upon the completion of this incubation period, the cultures were removed for quantification of the surviving colonies. The variation in the number of CFUs before and after the 30-minute exposure to the test surfaces served as a measure of the intensity of the biocidal effect.

RESULTS AND DISCUSSION

The average roughness (Ra) value recorded in the direction parallel to the grooves created by the additive manufacturing process was 6.58 ± 1.09 µm. In the direction perpendicular to the grooves, the average roughness value was 22.51 ± 1.19 µm. When the PLA plates were coated solely with varnish, a decrease in Ra values for both directions was observed: 4.36 ± 0.81 µm and 18.10 ± 0.67 µm, respectively. This equates to a reduction in roughness of the varnish-coated plate by approximately 19.6% in the perpendicular direction and 33.7% in the direction parallel to the deposition lines. This result suggests that the varnish served to fill the surface cavities and reduce the material's overall roughness, and that it has an average thickness of at least of the order of 2 µm.

Figures 2, 3, 4, and 5, illustrate the roughness profiles derived from the surfaces of the PLA plates, both without any coating and those solely coated with varnish. The results revealed a pronounced anisotropy in the surface morphology for the evaluated directions offset by 90 degrees, in both instances. Ra values were roughly threefold higher when measured perpendicular to the printing direction. This is attributable to the parameters employed in the additive manufacturing process, which has a preferred direction for material deposition, commonly referred to as printing lines [26].

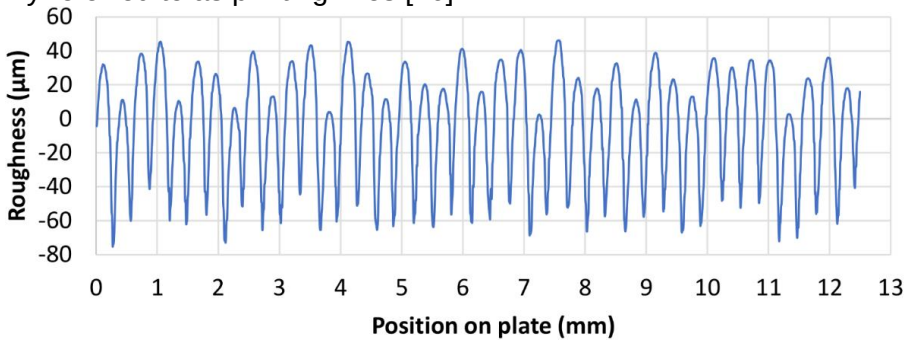

Figure 2. Roughness profile for uncoated PLA plate - measurement perpendicular to the printing lines.

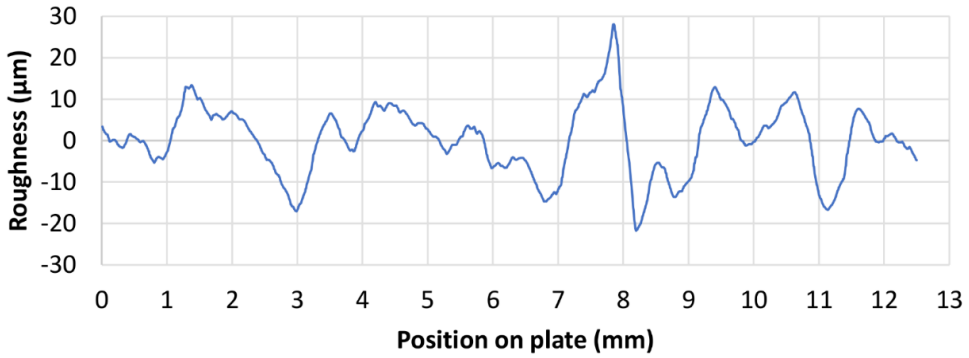

Figure 3. Roughness profile for uncoated PLA plate - measurement parallel to the printing lines.

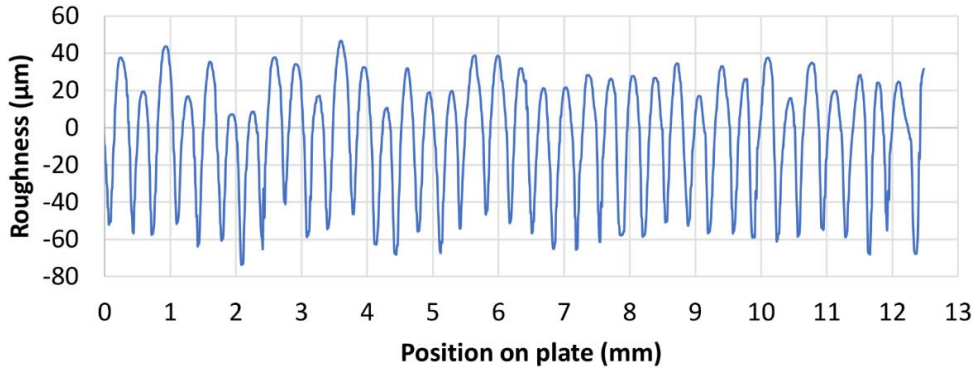

Figure 4. Roughness profile for PLA plate coated with varnish - measurement perpendicular to the printing lines.

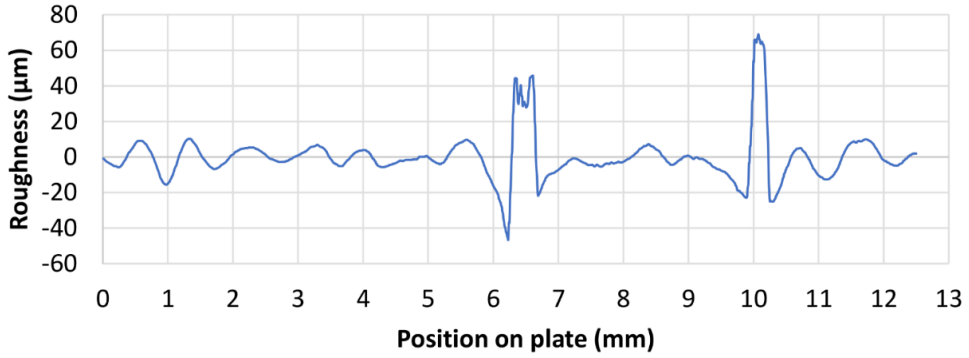

Figure 5. Roughness profile for PLA plate coated with varnish - measurement perpendicular to the printing lines.

Figure 6 displays the morphology of the PLA surface, as observed through OM following the application of the sealant. The image prominently features parallel printing lines, a byproduct of the manufacturing process. The silver nitrate crystals, which are transparent and adhered to the surface during the curing of the varnish, exhibited varied sizes. In certain areas, they formed randomly distributed clusters. Moreover, the manual application of the sealant using a brush may have contributed to the preferential accumulation of larger particles at the edges of some samples, as depicted in the figure. This phenomenon could be related to the direction used to cover the PLA, especially if the brushing action during manual application favors the alignment with or perpendicularity to the printing lines. In addition, the transparency of the sealant facilitates the clear visibility of the silver nitrate crystals and 3D printing grooves as seen in Figure 6.

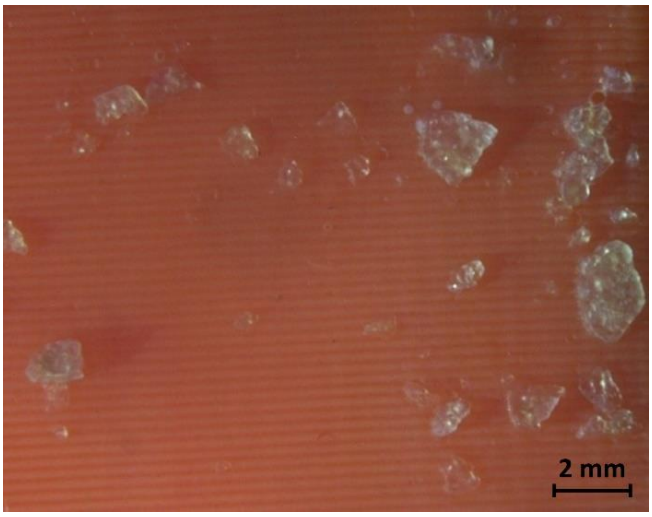

Figure 6. Surface of PLA printed by additive manufacturing and adhered silver nitrate crystals.

The application of the quantitative stereology technique [27] in conjunction with Digital Image Processing (DIP) indicated an area fraction (AA) of 12% for the silver nitrate crystals. This result can be attributed to the manual application of the sealant and the granulometry of the silver nitrate crystals, which were used as received, without any comminution. Figure 7 provides an illustration of the results obtained for the AA (%) occupied by the silver nitrate.

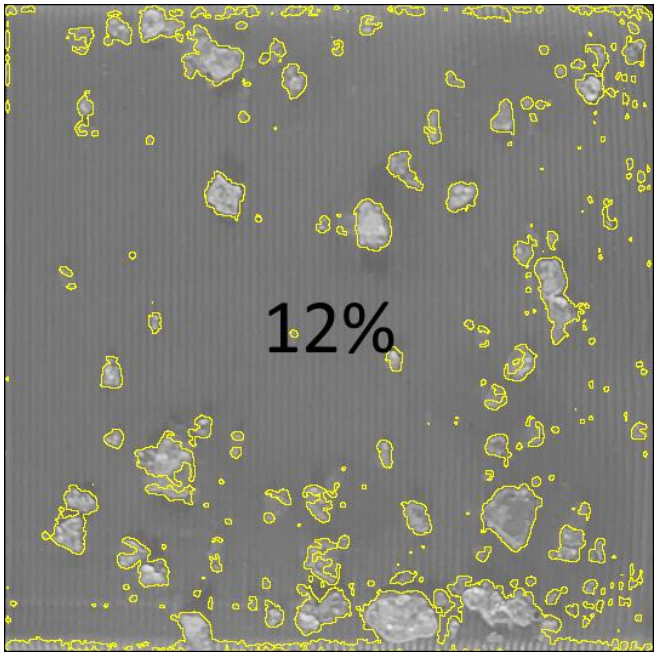

Figure 7. Image of a plate coated with sealant and used for the DIP.

Figure 8 exhibits an image obtained via SEM in BSE mode. This particular mode is employed to identify regions of varied chemical composition within the material. Areas appearing in lighter or darker shades indicate the presence of chemical elements with higher or lower atomic weights, respectively [15]. The images derived from all examined regions exhibited uniform shades of gray, suggesting a consistent chemical compound present across the surface of the plates. The silver nitrate crystals appeared to be encapsulated and adequately coated by the varnish, as the presence of silver was not detected by the technique. The maximum detection depth of the analysis performed, which is on the order of 1 µm, did not penetrate the varnish layer encapsulating the silver nitrate crystals.

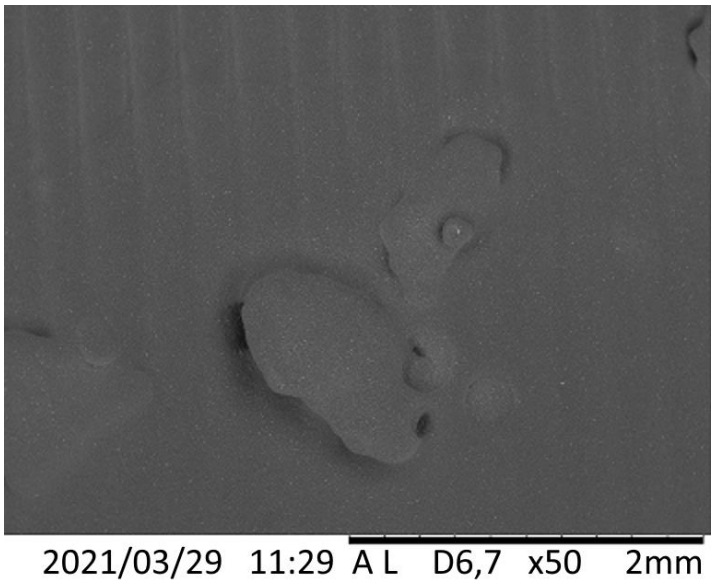

Figure 8. Image of a surface coated with the sealant obtained by SEM in BSE mode. The silver nitrate crystals are evidenced only by relief, but not by chemical composition.

The characteristic energy spectra obtained through EDS technique primarily indicated the presence of carbon and silicon. This was expected as these elements are commonly found in varnishes [28]. Silver, an element that is easy to detect due to its higher atomic weight compared to carbon and silicon, was not identified. This evidence suggests that the metallic crystals were thoroughly encapsulated and that the thickness of the varnish coating on the silver-containing crystals exceeded the detection limit of the equipment [15]. Figures 9 (a) and 9 (b) show a region of the plate surface coated with the sealant containing silver nitrate crystals. This region was subject to chemical microanalysis via EDS. The resulting characteristic energy spectrum identified only the peaks corresponding to silicon, oxygen, and carbon.

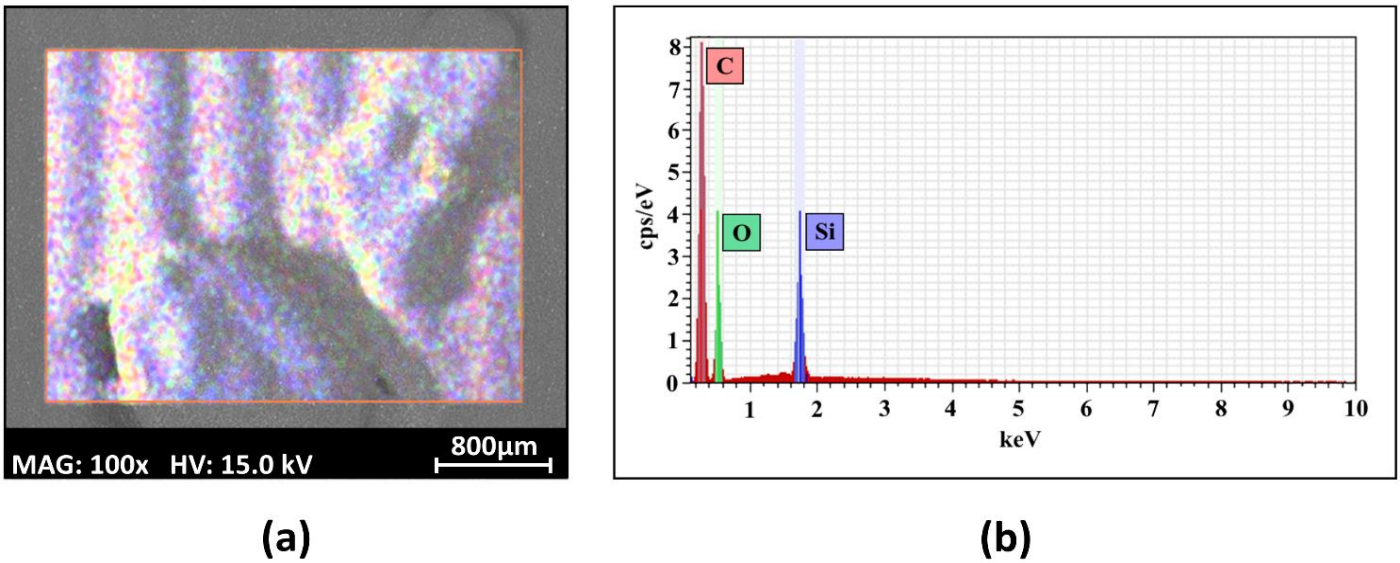

Figure 9. a) Analyzed region; b) Characteristic energy spectrum obtained for the region shown in Figure 10 (a).

For the evaluation of the sealant's cross-section, samples were dipped in liquid nitrogen and subjected to brittle fracture. This method ensures that the sealant layer's morphological structure isn't altered by typical sample preparation procedures [29]. Figure 10 presents one of the obtained aspects for the sealant's cross-section, where micropores with diameters ranging from 10-30 µm were identified. Figure 11 shows the location where the sealant layer was analyzed and indicates the presence of pores between the layers of PLA deposited during the additive manufacturing process. These pores could potentially serve as a refuge for bacteria or other microorganisms, highlighting the importance of thorough sealing.

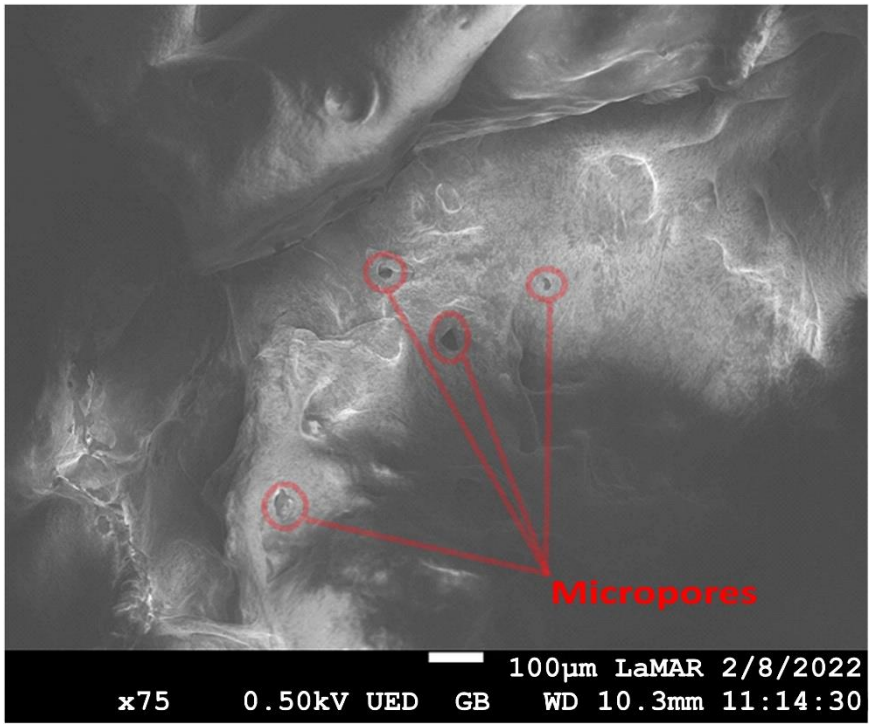

Figure 10. Cross-section of the sealant that covered the PLA - micropores.

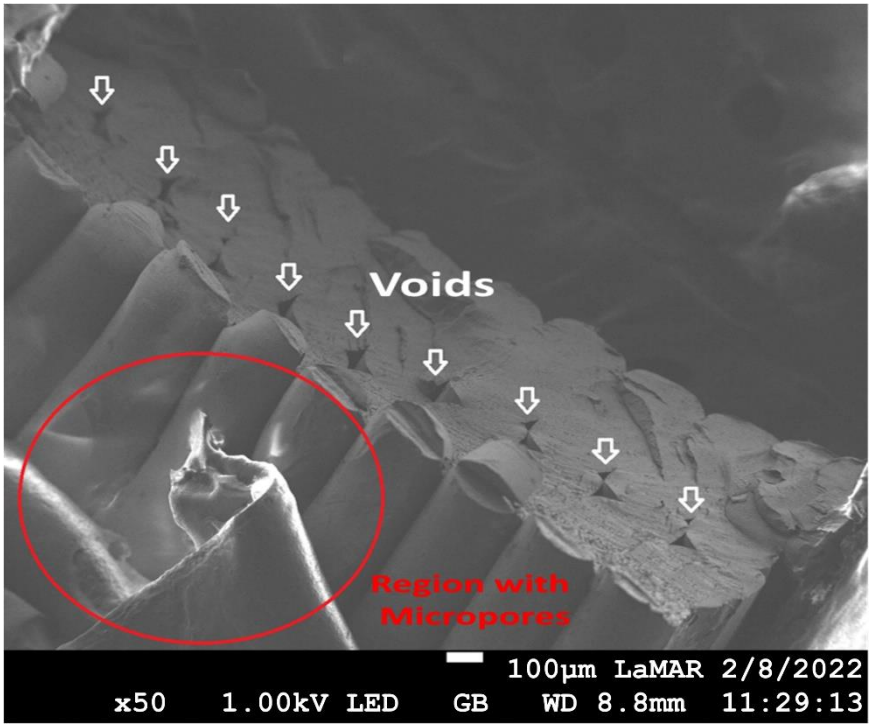

Figure 11. Cross-section of the printed PLA plate: Layer of sealant analyzed in Figure 11 (highlighted in red) and pores generated during layer deposition (arrows).

Figures 12 and 13 display the results from the *in vitro* tests, offering a comparison for analyzing the biocidal effect of the sealant against *Escherichia coli* ATCC 11229 and *Staphylococcus aureus* ATCC 25923. These graphs show the amount of the initial inoculum and the quantity recovered after a 30-minute contact period with all the tested surfaces, following which bacteria were gently brushed off.

For *Escherichia coli* ATCC 11229, there was a complete elimination of microorganisms, indicating that the sealant effectively killed this bacterial strain. This is a significant finding, given the prevalence and potential health impacts of E. coli. In the case of *Staphylococcus aureus* ATCC 25923, the results showed a substantial reduction in the number of CFUs, as it reduced bacterial presence on treated surfaces by a factor

of 64 compared to untreated ones. This suggests that the sealant also has a strong biocidal effect against S. aureus, another common and potentially harmful bacterium.

Additionally, Figures 12 and 13 also highlight that when used alone, varnish did not demonstrate significant bactericidal effects. While it served effectively as a sealant, it did not present inherent antimicrobial properties when applied to the PLA plates. When comparing the pure PLA plates with the varnish-coated ones, the recovered bacterial quantities were at the same order of magnitude for both *Escherichia coli* ATCC 11229 and *Staphylococcus aureus* ATCC 25923. This was particularly noticeable with *Staphylococcus aureus* ATCC 25923, where the recovery numbers were 5,300 and 5,200 CFUs, respectively. This clear evidence suggests that the varnish by itself does not confer any antibacterial properties and confirms the necessity of silver nitrate crystals for the sealant's antimicrobial action.

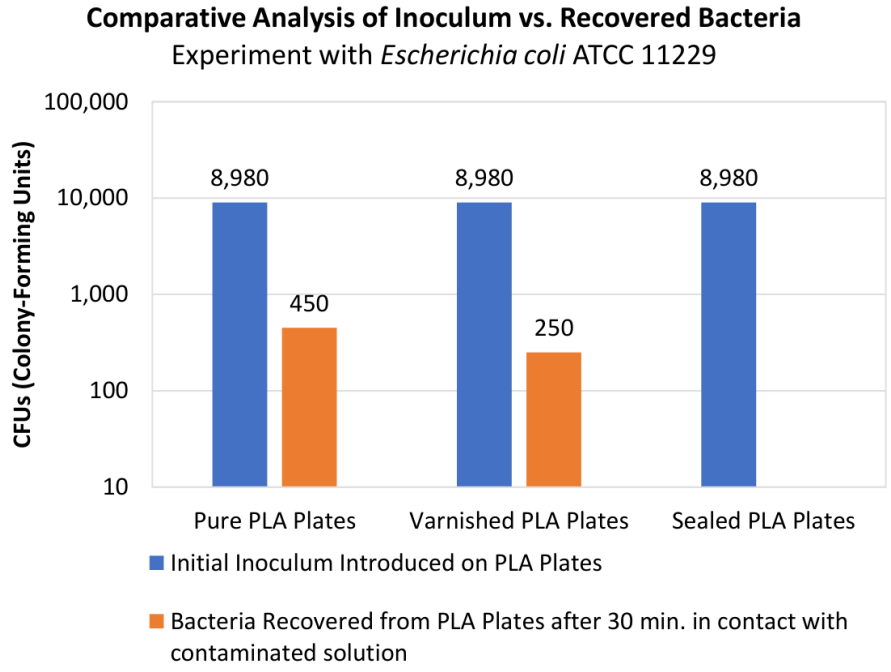

Figure 12. Comparative chart between the inoculum of *Escherichia coli* ATCC 11229 and the bacteria recovered on plates without coating, with varnish, and with sealant.

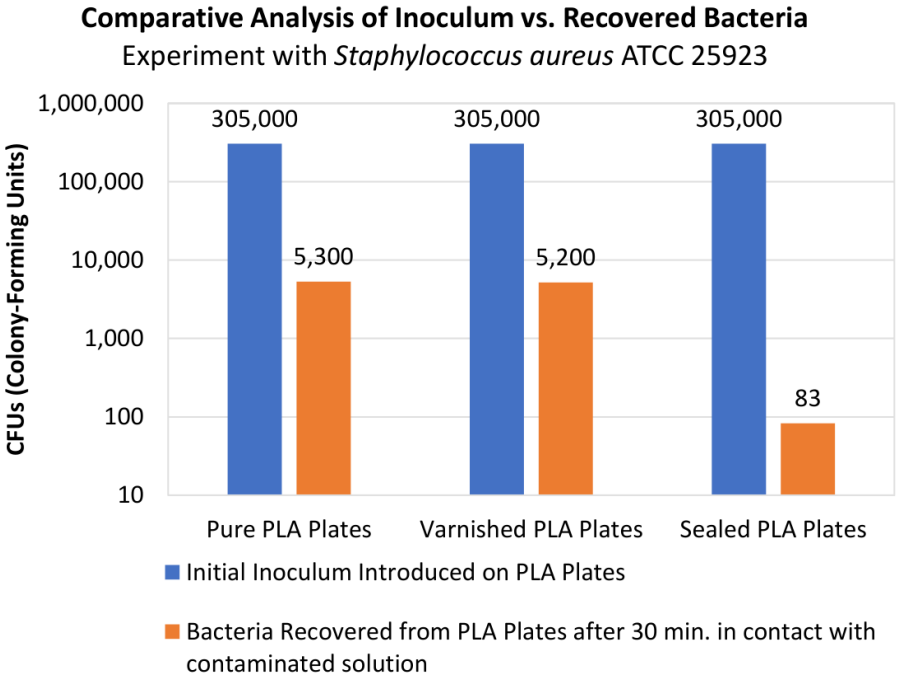

Figure 13. Comparative graph between the inoculum of *Staphylococcus aureus* ATCC 25923 and the bacteria recovered on plates without coating, with varnish, and with sealant.

The observed change in surface finish resulting from the varnish application on the PLA plates produced via additive manufacturing, marked by the difference in Ra between the pure plate and the varnish-coated plate (roughness reduction of around 19.6% in the perpendicular direction and 33.7% parallel to the printing lines), did not significantly influence the outcomes of the *in vitro* tests. The number of bacteria recovered after brushing the varnish-only and uncoated plates was similar, suggesting that the roughness variation did not alter bacterial adhesion or survival rates. It is known that the morphology and surface finish of materials can influence cell survival and proliferation [24,30].

The bactericidal efficacy of silver was corroborated in the system tested, consistent with prior studies [10,31]. The mechanism by which silver nitrate interacts with bacteria and viruses, leading to their inactivation or demise, is well-established in the field of microbiology. Silver ions, released from silver nitrate, interfere with the vital metabolic processes of these microorganisms, disrupting their normal functioning. Additionally, these ions are known to bind with the DNA of the bacteria or viruses, preventing its replication and thereby, effectively halting the proliferation of the microorganisms. The existence of micropores within the sealant layer (as illustrated in Figure 10) appears to have served as conduits for the release of silver ions between the encapsulated silver nitrate crystals and the external environment housing the bacterial colonies. Despite the clusters of crystals carrying the biocidal agent being enclosed within the varnish, these interconnected micropores could have facilitated the diffusion of silver ions, which are known to possess antimicrobial properties, into the bacterial environment. Hence, the design of this sealant system seems to effectively harness the bactericidal potential of silver nitrate, showcasing its potential for use in various applications where antimicrobial surfaces are desired.

CONCLUSION

The current study thoroughly investigated the properties of Polylactic Acid (PLA) surfaces produced by additive manufacturing and their interactions with bacterial colonies when coated with a varnish-based sealant containing silver nitrate crystals. The approach encompassed a broad range of techniques: from visual examination and average roughness (Ra) calculations to advanced methods such as optical microscopy (OM), digital image processing (DIP), scanning electron microscopy (SEM), and energy dispersive spectroscopy (EDS) for semi-quantitative chemical analysis. Furthermore, *in vitro* tests were conducted to measure the biocidal performance of the sealed PLA plates.

From a surface characterization perspective, the study revealed the surface of the printed PLA had anisotropic characteristics and that its coating with the varnish, which was the sealant matrix, caused a reduction in roughness. Moreover, despite 12% of the surface area of the plates was occupied by silver nitrate crystals, these crystals remained undetectable by the EDS technique, indicating that they were effectively encapsulated by the varnish. Micropores were found in the cross-section of the sealant layer analysis. This microporous structure presumably served as a conduit for silver ions, released from the silver nitrate, to interact with the external environment and exert their bactericidal effect on bacterial colonies, even though the silver nitrate was fully covered by varnish.

One of the primary advantages of this approach lies in its efficiency. The usage of minimal silver nitrate to achieve potent antimicrobial effects underscores its cost-effectiveness. This efficiency also mitigates any potential environmental concerns linked to the excessive use of silver compounds. Additionally, the flexibility of this method is an important feature, suggesting that it could be extended to other types of materials and surfaces, thereby broadening the range of its beneficial antimicrobial impacts.

The sealant demonstrated significant antimicrobial action, causing reduction of at least 64 times in the number of bacteria initially inoculated on the sealant-coated surfaces, within just 30 minutes of contact, when compared to the bacterial count on uncoated surfaces. This study conclusively demonstrated the potent bactericidal effect of silver on *Escherichia coli* ATCC 11229 and *Staphylococcus aureus* ATCC 25923. This effect occurred despite the anisotropy of the surface created by additive manufacturing, indicating the potential of such sealant systems for practical antimicrobial applications. Remarkably, the effectiveness of the antimicrobial action was maintained despite the surface anisotropy inherent to the additive manufacturing process, underscoring the applicability of such sealant formulations in real-world antimicrobial scenarios across diverse sectors, such as healthcare, food packaging, and water treatment. However, further testing is required to fully understand the scope and limitations of this sealant's antimicrobial action.

Funding: This study received financial support from the Coordination for the Improvement of Higher Education Personnel - CAPES (Grants 88887.708586/2022-00 and 88881.708587/2022-01) and Carlos Chagas Filho Research Support Foundation of the State of Rio de Janeiro - FAPERJ (Grants E-26/201.344/2022 and E-26/210.206/2020).
Conflicts of Interest: The authors declare no conflict of interest. The funders had no role in the design of the study; in the collection, analyses, or interpretation of data; in the writing of the manuscript, or in the decision to publish the results.

REFERENCES

1. Nelson KE, Williams CM. Infectious disease epidemiology: theory and practice. Burlington, MA (USA): Jones & Bartlett Learning; 2014. 963 p.
2. De La Rosa M, Prieto JP. [Microbiology in Health Sciences: Concepts and Applications]. 3rd ed. Barcelona (Spain): Elsevier; 2011. 384 p.
3. Woźniak-Budych MJ, Przysiecka Ł, Langer K, Peplińska B, Jarek M, Wiesner M, et al. Green synthesis of rifampicin-loaded copper nanoparticles with enhanced antimicrobial activity. J Mater Sci Mater Med. 2017; 28(3):1-6. doi:10.1007/s10856-017-5857-z.
4. Zhuang Y, Zhang S, Yang K, Ren L, Dai K. Antibacterial activity of copper-bearing 316L stainless steel for the prevention of implant-related infection. J Biomed Mater Res B Appl Biomater. 2020;108(2):484-95. doi:10.1002/jbm.b.34405.
5. Valero PL. [Nanostructured Inorganic Materials Based on Silver: Bactericidal Applications] [PhD Thesis]. Zaragoza: Universidad de Zaragoza; 2013. 216 p.
6. Cao W, Zhang Y, Wang X, Chen Y, Li Q, Xing X, et al. Development of a novel resin-based dental material with dual biocidal modes and sustained release of Ag+ ions based on photocurable core-shell AgBr/cationic polymer nanocomposites. J Mater Sci Mater Med. 2017; 28(7):01-11. doi:10.1007/s10856-017-5918-3.
7. Tanikella NG, Wittbrodt B, Pearce JM. Tensile strength of commercial polymer materials for fused filament fabrication 3D printing. Addit Manuf. 2017; 15:40-7. doi:10.1016/j.addma.2017.03.005.
8. Amousoltani N, Salimijazi H, Golozar M. Study of alumina sealing of HVOF thermally sprayed WC-Co coatings by sol-gel method. Mater Res Express. 2019; 7(1):016410. doi:10.1088/2053-1591/ab5fea.
9. Simmons J. Antimicrobial additive systems see increased use in polymers. Plast Addit Compd. 2001; 3(12):16-8. doi:10.1016/S1464-391X(01)80329-9.
10. Mendes E, Mendes E, Savi GD, Angioletto E, Riella HG, Fiori MA. High performance bactericidal glass: evaluation of the particle size and silver nitrate concentration effect in ionic exchange process. Ceram. 2018; 64:156-65. doi:10.1590/0366-69132018643702197.
11. Regí MV. [Biomaterials for Tissue Replacement and Repair by the Spanish Association of Scientists]. Asociación Española de Científicos [Internet]. 2004 [cited Jun. 19, 2023]. Available from: https://www.aecientificos.es/biomateriales-para-sustitucion-y-reparacion-de-tejidos.
12. Associação Brasileira de Normas Técnicas. ABNT NBR ISO 4287:2002 Especificações geométricas do produto (GPS)-Rugosidade: Método do perfil-Termos, definições e parâmetros da rugosidade [Geometric Product Specifications (GPS) - Roughness: Profile Method - Terms, Definitions, and Roughness Parameters]. Associação Brasileira de Normas Técnicas. 2002.
13. Associação Brasileira de Normas Técnicas. ABNT NBR ISO 4288:2008. [Geometric Product Specifications (GPS) - Roughness: Profile Method - Rules and Procedures for the Evaluation of Roughness]. 2008.
14. Luiz VD, Amaral EC, Souza VP, Rodrigues PC. [Influence of Stamping Speed and Anisotropy on the Tribological Behavior and Fracture of an AISI 430Nb Steel Sheet]. Matéria (Rio J.). 2022;27(1). Doi:10.1590/1517-7076-RMAT-2021-48196.
15. Goldstein JI, Newbury DE, Michael JR, Ritchie NW, Scott JH, Joy DC. Scanning electron microscopy and X-ray microanalysis. springer; 4th ed. New York (NY): Springer; 2017. 550 p. doi:10.1007/978-1-4939-6676-9.
16. Gonzalez RC, Woods RE. Digital image processing, 3rd ed. Upper Saddle River (NJ): Prentice Hall, 2008. 954 p.
17. Malacara D. Color vision and colorimetry: theory and applications, 2nd ed. Bellingham (WA): SPIE,2011.175p.
18. Splittstoesser DS, Downes FP, Ito K, Vandezant C. Compendium of methods for the microbiological examination of foods, 4th ed. Washington (DC): American Public Health Association, 2001. 676 p.
19. Lennette EH. Manual of clinical microbiology, 4th ed. Washington (DC): American Society for Microbiology, 1985. 1149 p.
20. Goldman E, Green LH. Practical handbook of microbiology, 2nd ed. Boca Raton (FL): CRC Press, 2009. 874 p.
21. Cockerill FR. Methods for dilution antimicrobial susceptibility tests for bacteria that grow aerobically: approved standard. 9th ed. Wayne (PA): Clinical and Laboratory Standards Institute; 2012. 68 p.
22. Chanes-Cuevas OA, Arellano-Sánchez U, Álvarez-Gayosso CA, Suaste-Olmos F, Villarreal-Ramírez E, Álvarez-Fregoso O, et al. Synthesis of PLA/SBA-15 composite scaffolds for bone tissue engineering. Mater Res. 2020; 23(5). doi:10.1590/1980-5373-MR-2020-0211.
23. Ferraz C, Rocha C, Rocha MM, Martins MD, Jacques P. Contaminação de resinas compostas na prática odontológica [Contamination of Composite Resins in Dental Practice]. Pesqui Bras Odontopediatria Clín Integr. 2010; 10(1):73-8. doi:10.4034/1519.0501.2010.0101.0012.
24. Diniz MG, Soares GA, Coelho MJ, Fernandes MH. Surface topography modulates the osteogenesis in human bone marrow cell cultures grown on titanium samples prepared by a combination of mechanical and acid treatments. J Mater Sci Mater Med. 2002; 13(4):421-32. doi: 10.1023/A:1014357122284.
25. López OMF, Apaza YCL. [Design of an Electronic UV Sterilization Chamber for Medical Protective Equipment Against COVID-19]. doi: 10.1590/SciELOPreprints.1105.

26. Volpato N. [Additive Manufacturing: Technologies and Applications of 3D Printing]. 1st ed. São Paulo (Brazil): Blucher; 2017. 400p.
27. Underwood EE. Quantitative stereology for microstructural analysis. Microstructural Analysis: Tools and Techniques. Boston (MA): Springer; 1973.35-66 p. doi: 10.1007/978-1-4615-8693-7_3.
28. Vazquez-Calvo C, De Buergo MA, Fort R, Varas MJ. Characterization of patinas by means of microscopic techniques. Mater Charact. 2007; 58(11-12):1119-32. doi:10.1016/j.matchar.2007.04.024.
29. Dedavid BA, Gomes CI, Machado G. [Scanning Electron Microscopy: Applications and Sample Preparation: Polymeric, Metallic, and Semiconductor Materials]. Porto Alegre (Brazil): EdiPUCRS; 2007. 60 p.
30. Coyle S, Doss B, Huo Y, Singh HR, Quinn D, Hsia KJ, et al. Cell alignment modulated by surface nano-topography–Roles of cell-matrix and cell-cell interactions. Acta Biomater. 2022; 142:149-59. doi:10.1016/j.actbio.2022.01.057.
31. Mirzajani F, Ghassempour A, Aliahmadi A, Esmaeili MA. Antibacterial effect of silver nanoparticles on Staphylococcus aureus. Res Microbiol. 2011; 162(5):542-9. doi:doi.org/10.1016/j.resmic.2011.04.009.